

# Principle behind droplet formation in microfluidic devices based on force balance

## Prinzip der Tröpfchenbildung in mikrofluidischen Geräten basierend auf Kräftegleichgewicht

Emil Grigorov

Technical University of Sofia, Faculty of German Engineering and Economics Education,  
Sofia, Bulgaria, e-mail: egrigorov@FDIBA.tu-sofia.bg

**Abstract** — The work presents a numerical study of the mechanisms responsible for the droplet formation in a flow-focusing microfluidic device. The three stages of droplet formation in the dripping regime and the responsible forces for their formation were analysed. Surface tension  $\Delta\sigma$ , the pressure difference between inside and outside of the droplet  $\Delta p_{\text{int}}$  and the shear stresses  $\tau_{x_i x_j}$  are taken into account as the main parameters responsible for droplet generation. The results show that the whole process is driven by a force disbalance. In the first stage of droplet formation, in which the droplet is growing in diameter, the surface tension is the domination force. The second stage however, in which the actual neck squeezing and droplet detachment occur, can be described by the increase of the outside channel pressure on the surface. This analyse was confirmed by the development of the neck diameter of the forming bubble.

**Zusammenfassung** — Die Arbeit präsentiert eine numerische Studie der Mechanismen, die für die Tröpfchenbildung in einem mikrofluidischen Gerät verantwortlich sind. Analysiert wurden die drei Stadien der Tropfenbildung im sogenannten Dripping regime und die verantwortlichen Kräfte für ihre Bildung. Als hauptsächlich verantwortliche Parameter werden die Oberflächenspannung  $\Delta\sigma$ , die Druckdifferenz zwischen dem Inneren und Äußeren des Tropfens  $\Delta p_{\text{int}}$  und die Schubspannungen  $\tau_{x_i x_j}$  berücksichtigt. Die Ergebnisse zeigen, dass der gesamte Prozess durch ein Kräfteungleichgewicht angetrieben wird. In der ersten Stufe der Tröpfchenbildung, in der der Tröpfchendurchmesser zunimmt, ist die Oberflächenspannung die dominierende Kraft. Die zweite Stufe jedoch, in der die eigentliche Halsquetschung und Tropfenablösung erfolgt, lässt sich durch die Erhöhung des Außenkanaldrucks auf der Oberfläche beschreiben. Diese Analyse wurde durch die Entwicklung des Halsdurchmessers der sich bildenden Blase bestätigt.

### I. INTRODUCTION

In recent years, microfluidics developed as a novel approach for solving numerous questions arising from the realization of different biological, chemical and medical processes [citeee]. Having fluidic channels with dimensions smaller than a millimetre, i.e. micro-scale, microfluidic devices can significantly reduce reaction times and energy consumption for a certain process [citeee]. The extremely low Reynolds number result in strictly laminar flow conditions in the channels and thus providing an absolute control over fluidic flows supply in different chip regions. With well-defined microenvironments which mimic the habitants of living cells, microfluidic devices enable the successful integration and replacement of expensive and demanding laboratory equipment in these small chips [citeee]. An emerging microfluidic technology based on hydrodynamics principles, utilized as a precise and reliable tool for the automation of assays is the so-called droplet-based microfluidics. Encapsulating different chemical or biological compounds into individual picolitre-droplets, allows the isolation of the occurring reactions from their surroundings, avoiding unwanted mixing and disruption of fragile compounds. These small microreactors allow a cheap and

easily implementable method for a broad range of processes including cell lysis [citeee], antibiotics susceptibility screening [cite], digital polymerase chain reaction (PCR) [citeee] etc. The massive number of possible independent reactions in the droplets adds also a high parallelization factor into the conducted experiments. Three main geometry types for droplet generation are widely utilized in the microfluidic world: co-flow of dispersed and continuous phases, cross-flow in T-junction and flow-focusing (Figure 1).

All of these potential advantages come at the price of a high hydrodynamic complexity of the microfluidic system due to the dynamic interaction between forces acting on the interface of the two phases. One of the phenomena characterizing these multiphase microfluidic flows and their complexity is the occurring of different flow regimes depending on the systems boundary conditions.

For the design of microfluidic devices operating in droplet flow regime, prior knowledge of droplet size, shape, formation frequency or pressure drop are essential.

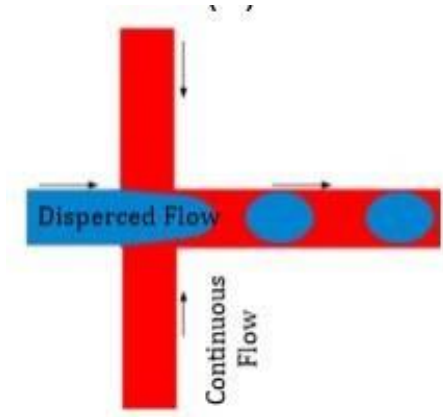


Fig. 1. Flow-focusing microfluidical setup for the droplet generation.

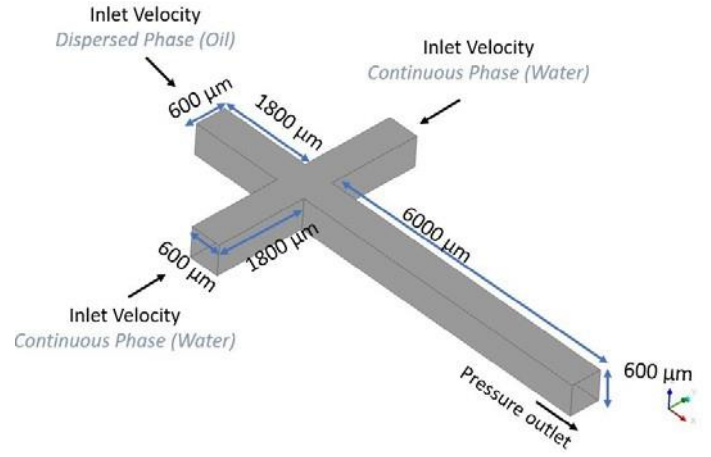


Fig. 2. Model geometry, dimensions and boundary conditions.

Even though the principles of droplet formation are well understood, there is, in our opinion still a lack of detailed explanation of the influence of the responsible parameters during the process. Although there are plenty of existing theoretical/experimental works for the flow-focusing geometry, there is a need to fill the gap between the limitations of the experimental measurements and theoretical assumptions, simplifying the problem. A good way to collect in advance this information for a new setup is by utilizing a predictive CFD (Computational Fluid Dynamics) model and interpreting the influences of some fluid properties on the droplet breakup. Few numerical studies on droplet-based microfluidics were carried out in the past years utilizing different numerical techniques (for example level set (LS) [11] or Lattice Boltzmann method (LBM) [12-13]). In this article we investigate numerically the droplet cause of bubble formation in a flow-focusing microfluidic channel by utilizing the volume of fluid (VOF) method. The three main pressures responsible for droplet formation are analysed. The mechanism behind droplet formation is described through a pressure (dis) balance.

## II. MATHEMATICAL MODEL, GEOMETRICAL SETUP AND BOUNDARY CONDITIONS

In the present study three-dimensional simulations of droplet formation in a flow-focusing geometry are carried out utilizing a finite volume method based CFD solver from ANSYS Fluent 21. The two immiscible fluids, water and oil as well as their interface, are modelled by the Volume of fluid (VOF) method. A phase fraction parameter,  $\alpha$ , is used to indicate the presence of each phase at every location of the domain. Fluid properties such as viscosity and density are smoothed and the surface tension force is distributed near the interface as a body force in the Navier-Stokes equations. With this, the system of coupled partial differential equation consists of the continuity equation (1) the momentum balance equation (2), and the phase fraction equation for  $\alpha$  (3) becomes [14]:

$$\frac{\partial \rho}{\partial t} + \nabla \cdot \rho \mathbf{U} = 0 \quad (1)$$

$$\frac{\partial (\rho \mathbf{U})}{\partial t} + \nabla \cdot (\rho \mathbf{U} \mathbf{U}) = -\nabla p + \nabla \cdot (\mu [\nabla \mathbf{U} + \nabla \mathbf{U}^T]) + \mathbf{F}_s \quad (2)$$

$$\frac{\partial \rho \alpha}{\partial t} + \nabla \cdot \rho \alpha \mathbf{U} = 0 \quad (3)$$

In the equations above,  $\mathbf{U}$  is the velocity vector field,  $p$  is the pressure field and  $\mu$  the viscosity of the fluid.  $\mathbf{F}_s$  represents the surface tension force, which can be calculated as follows:

$$\mathbf{F}_s = \sigma \cdot \kappa(\nabla \alpha) = \sigma \cdot \nabla \cdot \left( \frac{\nabla \alpha}{|\nabla \alpha|} \right) \cdot (\nabla \alpha) \quad (4)$$

$\kappa$  describes the curvature of the interface between the fluids. Only one such transport equation (3) needs to be solved since the volume fraction of the other phase can be inferred from the constraint:

$$\alpha_c + \alpha_d = 1 \quad (5)$$

where the index 'c' stands for continuous and 'd' for dispersed phase. The continuous phase (water) is introduced through the two side channels and the dispersed phase (oil: octane +2,5 % SPAN 80) is entered from the main (central) channel. The information about the fluid properties is obtained from the experimental results of Yao et al. [15]. All the measurements were conducted under atmospheric pressure conditions and room temperature.

TABLE I. SUMMARY OF THE FLUID PROPERTIES

Fluid	Density $\rho$ - [kg m <sup>-3</sup> ]	Viscosity $\mu$ - [mPa s]
Water	1004,4	3,32
Oil	689,9	0,53

For the boundary conditions, constant velocity block profile was utilized for both continuous and dispersed phase inlets. We set  $\alpha = 1$  at the inlet of the dispersed phase and  $\alpha = 0$  at the inlet of the continuous phase. No slip boundary conditions are applied at the walls. Pressure boundary was specified at the outlet of the main channel. The inlet velocities of both fluids were kept equal at  $u_d = 0,00925 \text{ m s}^{-1}$  for the simulated case. The surface tension coefficient between the two fluids is  $\sigma = 5,04 \text{ mN m}^{-1}$ . The lengths and dimensions of the square cross-section, the inlet and outlet channels are presented in Figure 2.

### III. CONSIDERED FORCES

In this section we describe the considered pressures (forces) on the interface between the two fluids, responsible for the droplet generation. The main pressure, which acts in the negative x-direction (trying to pull back the forming bubble) is the surface tension:

$$\Delta p_{\sigma} = \sigma/\kappa \quad (6)$$

In our analysis the value of  $\kappa$  are directly taken from Equation 4 precisely from the Fluent Solver, which is directly accessible in the post processing stage. When the fluids are at rest and for perfect geometries of the interface (sphere, cylinder etc.) this pressure force is balanced by the pressure difference through the interface:

$$\Delta p_{int} = p_i - p_o \quad (7)$$

In our case  $p_i$  is always defined as the static pressure inside the droplet, whereas  $p_o$  is the static pressure of the surrounding continuous phase, entering the domain through the two side channels.

When the two fluids move in the microchannel, the above-mentioned forces will deviate from these theoretical values. At this point it is important to take into account the influence of the forces acting in tangential direction of a fluid element. For an isotropic Newtonian fluid, the viscous stress tensor can be defined as follows:

$$\tau_{x_i x_j} = \mu_c \cdot \frac{\partial v_i}{\partial x_j} + \frac{\partial v_j}{\partial x_i} \quad (8)$$

In the present work we decided to do the analysis using local values available from the computations. Definition of forces would require to define also the exact areas these forces work on which would present rather global (as opposed to local) quantities. Most often the local parameters available from the numerical method are in terms of normal and tangential stresses with dimension Pa. That is the reason to define also  $\Delta p_{\sigma}$ .

### IV. RESULTS

In this work only the so-called dripping regime is discussed. The latter is characterised by bigger emulsions and relative low detachment frequency, as shown in a work [1]. The process of droplet detachment is marked by three main stages, as visible on the normalized neck (DD) of the advancing oil front, as shown in Figure 3. First, the so-called filling stage is observed, where the dispersed phase is injected into the cross section for a time of  $t_{fill}$ . The diameter of the forming bubble becomes larger than the width of the channel. At some point the dispersed flow almost blocks the flow from the side channels, causing the upstream pressure to increase, see Figure 1b. In a second stage starting from  $t = 0,109$  s the diameter of the droplet starts to reduce, becoming smaller than the width of the channel, as shown for  $t = 119$  s. This stage is known as necking stage. At the beginning of this second phase the pressure in the side channel continuously increasing until  $t = 0,123$  s. One can see that the total increase in the side channels pressure is above 17 Pa, which obviously will result in a pressure increase at the interface. In the last pinch-off stage, droplet detaching occurs, marked in Figure 3 by the black arrow.

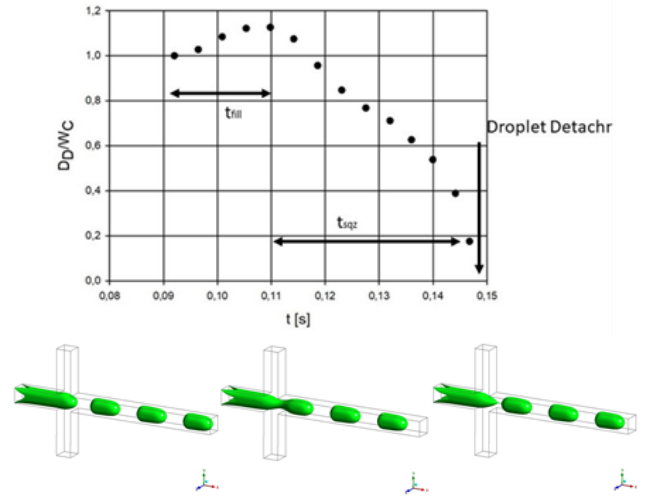


Fig. 3. The nondimensional diameter of the forming droplet as a function time and the iso-surfaces of the three stages (filling on the left, neck squeezing in the middle and droplet detachment on the right).

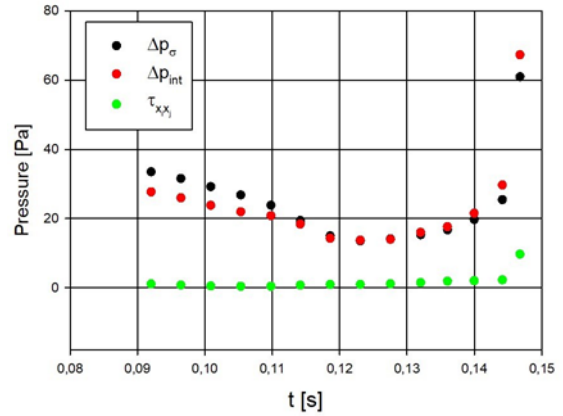


Fig. 4. Time development of the pressures, responsible for the droplet detachment.

This whole process characterizing the droplet formation in the dripping regime can be explained by the development of the pressure force caused by surface tension and the pressure difference through the interface, described in the previous section. Figure 4 shows the time development of the three pressures on the neck of the oil front. The effect of the shear stresses here is rather negligible. Comparing Figures 3 and 4 clearly shows that the whole process of droplet dormation is characterized by a disbalance between the interposing pressures. The domination of  $\Delta p_{\sigma}$  on the growing bubble at the beginning determines the growth in diameter of the propagating front. With time the two pressures reach a point of balance (for  $t$  around 0,0095 s), characterizing the end of this filling stage. From this moment on  $\Delta p_{int}$  begins to dominate over  $\Delta p_{\sigma}$ , giving start of the squeezing of the droplet neck.

As visible from Figure 5 the main cause for the starting decrease of the pressure difference between inside and outside of the bubble is attributed mostly to the increase in the pressure outside the bubble (at  $\alpha = 0,02$ ). The latter is attributed to the flow stagnation in the side chanel due to the propagation of the oil front. In the second part of the process one can see that the pressure in the side channel (outside the oil front) begins to decrease rapidly. This is attributed to the fact that the squeezing of the droplet neck is linked to a pressure release.

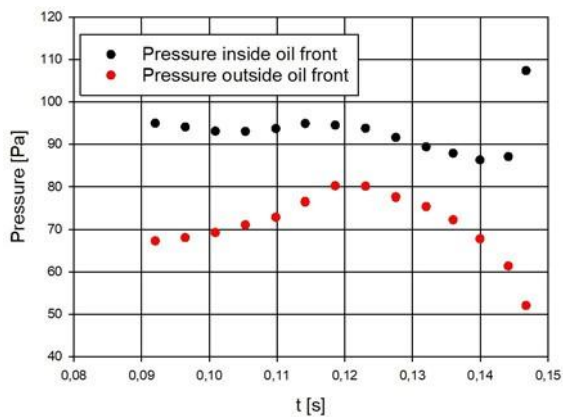


Fig. 5. Time development of the pressures inside and outside of the developing front of the dispersed face.

## V. CONCLUSION

In this work the droplet generation in a flow-focusing microfluidic device has been investigated. The continuous phase (water) was introduced through the two side channels and the dispersed phase (oil: octane +2,5 % SPAN 80) was entered from the main channel. For all simulations the VOF method was utilized. For the first time in the literature the responsible pressures for the droplet generation were described numerically. The surface tension, pressure difference between inside and outside of the forming bubble, and the shear stresses were considered for this analysis. It was shown that at the first stage of droplet generation, also known as filling stage, the surface tension dominates the two other forces, trying to minimize the area between the two fluids and thus increasing the diameter of the forming bubble. At some point the pressures in the two side channels increase, due to the stagnation of fluid flow there, thus increasing the influence of the outer pressures on the surface of the forming droplet. This increase of  $\Delta p$  in time overcomes the surface tension, giving begin to the second stage of droplet formation. This necking stage finishes with the final droplet detachment. The effect of the shear stresses on the surface were rather negligible, compared to the two other forces. As a whole, the present study shows that the VOF method is also a reliable technique for the simulation and prediction of droplet generation in a flow-focusing channels. It will allow the future study of other diverse setups and various fluid combinations.

## REFERENCES

- [1] N. Nguyen and S. Wereley, *Fundamentals and Applications of Microfluidics*; Artech House Publishing; Norwood, MA, USA, (2007), 3rd ed. Harlow, England: Addison-Wesley,
- [2] E. Grigorov, B. Kirov, M. Marinov and V. Galabov *Review of Microfluidic Methods for Cellular Lysis*, vol. 12, *Micromachines* 2021, 498
- [3] Y. Xu, Z. Zhang, Z. Zhou, X. Han and X. Liu, *Continuous Microfluidic Purification of DNA Using Magnetophoresis*, vol. 11, *Micromachines* 2020, 187
- [4] B. K. Madhusudan, G. Sanket, *Advances in continuous-flow based microfluidic PCR devices—a review*, vol. 2, *Eng. Res. Express* 2020, 042001
- [5] N. Shembekar, C. Chaipan, R. Utharala and C. A. Merten *Droplet-based microfluidics in drug discovery, transcriptomics and high-throughput molecular genetics*, vol. 16, *Lab Chip* 2016, 1314-1331
- [6] T. Thorsen, R. W. Roberts, F. H. Arnold and S. R. Quake *Dynamic Pattern Formation in a Vesicle-Generating Microfluidic Device*, vol. 86, *Phys. Rev. Lett.* 2001, 4163–4166
- [7] W. Zeng and H. Fu *Precise droplet formation in a T-junction microdroplet generator*, vol. 86, *IEE 8th International Conference on Fluid Power and Mechatronics (FP M) 2019*, 1190-1196
- [8] S. L. Anna, N. Bontoux and H. A. Stone *Formation of dispersions using “flow focusing” in microchannels*, vol. 82, *Appl. Phys. Lett.* 2003, 364–366
- [9] L. Yobas, S. Martens, W. L. Ong and N. Ranganathan *High-performance flow-focusing geometry for spontaneous generation of monodispersed droplets*, vol. 6, *Lab Chip* 2006, 1073–1079
- [10] C. Cramer, P. Fischer and E. J. Windhab *Drop formation in a co-flowing ambient fluid*, vol. 59, *Chem. Eng. Sci.* 2004, 3045–3058
- [11] W. Lan, S. Li, Y. Wang and G. Luo *CFD Simulation of Droplet Formation in Microchannels by a Modified Level Set Method*, vol. 53, *Ind. Eng. Chem. Res.* 2014, 4913
- [12] Y. Li, M. Jain, Y. Ma and Nandakumar *Control of the breakup process of viscous droplets by an external electric field inside a microfluidic device.*, vol. 11, *Soft Matter* 2015, 3884
- [13] A. Gupta, H. S. Matharoo, D. Makkar and R. Kumar *Geometry Effects of Axisymmetric Flow-Focusing Microchannels for Single Cell Encapsulation*, vol. 100, *Comput. Fluids* 2018, 218
- [14] C. Yao, Y. Liu, C. Xu, S. Zhao and G. Chen, *Formation of Liquid-Liquid Slug Flow in a Microfluidic T-junction: Effects of Fluid Properties and Leakage Flow*, vol. 64, *AIChE J.* 2018, 346
- [15] K. Ghaib *The Volume of Fluid Method, a Method for the Simulation of Two-Phase Flow*, *Chemie Ingenieur Technik* 2018, 316-323
- [16] L. Wu, M. Tsutahara, L. S. Kim and M. Ha, *Three-dimensional lattice Boltzmann simulations of droplet formation in a cross-junction microchannel*, vol. 34, *Int. J. Multiphase Flow* 2008, 852
- [17] P. A. Romero and A. R. Abate *Flow focusing geometry generates droplets through a plug and squeeze mechanism*, vol. 12, *Lab Chip* 2012, 5130-5132
- [18] X. Chen, T. Glawdel and N. Cui *Advances in Droplet-Based Microfluidic Technology and Its Applications*, vol. 18, *Microfluid Nanofluid* 2015, 1341–1353